Journal of Sound and Vibration (2000) **236**(5), 861–880
doi:10.1006/jsvi.2000.3040, available online at http://www.idealibrary.com on IDEAL®

ACTIVE WAVE CONTROL OF THE AXIALLY MOVING STRING: THEORY AND EXPERIMENT

C. A. TAN AND S. YING†

Department of Mechanical Engineering, Wayne State University, Detroit, Michigan 48202, *U.S.A.*
E-mail: tan@tan.eng.wayne.edu.

(*Received* 18 *June* 1999, *and in final form* 16 *March* 2000)

The active wave control of the linear, axially moving string with general boundary conditions is presented in this paper. Considerations of general boundary conditions are important from both practical and experimental viewpoints. The active control law is established by employing the idea of wave cancellation. An exact, closed-form expression for the transverse response of the controlled system, consisting of the flexible structure, the wave controller, and the sensing and actuating devices, is derived in the frequency domain. Two actuation forces, one upstream and one downstream of an excitation force, are applied. The proposed control law shows that all modes of the string are controlled and the vibration in the regions upstream and downstream of the control forces can be cancelled. However, these results are based on ideal conditions and the assumption of zero initial conditions at the non-fixed boundaries. Effects of non-zero boundary motions at the instant of application of the control forces are examined and the control is shown to be effective under these conditions. The stability and robustness of the control forces are improved by the introduction of a stabilization coefficient in the control law. The effectiveness, robustness and stability of the control forces are demonstrated by simulations and verified by experiments on axially moving belt drive and chain drive systems.

1. INTRODUCTION

The traveling string supported by two eyelets represents a simple and yet useful model that has been employed for a long time to describe the dynamics of machine elements for transmitting power, materials, or information [1]. Applications for this class of mechanical systems include chain and belt drives, band saws, magnetic tapes, and paper webs [2–4] which are collectively termed *axially moving materials*. Despite the many advantages of this machine element, noise and vibration associated with its motion have limited its utility in applications, in particular in high-speed operations, and when lighter and higher quality materials are required. For high-speed and precision applications, it is thus desirable to introduce suitable control methods to attenuate the vibration of the translating element in order to improve its performance.

Vibration control of flexible structures can be introduced by either passive or active methods, or a combination [5]. Techniques of active control are traditionally based on direct feedback control [6] and modal control [7] which models a continuous system by finite degrees of freedom or modes. The uncontrolled or residual modes can then destabilize the system via a spillover effect [7]. Because of this limitation, the feedforward control

†Currently at Ford Motor Company, Dearborn, MI, U.S.A.

0022-460X/00/400861 + 20 $35.00/0

approach [8] was proposed. The idea is to superimpose a secondary source on the primary excitation to cancel or absorb the travelling waves in the structure [9–14]. This active control scheme has its origin in sound reduction [15] and has been adopted in various vibration and noise control applications [8, 16]. The advantages of this technique are: (1) the control is free from the spillover effect and all modes can be controlled [9, 11], (2) the controller is suitable for vibration suppression away from the excitation force. However, it has been shown for the one-dimensional wave equation that the feedforward control is not robust and can be unstable if there are errors in the measurements [11]. Control of travelling waves in large space structures was examined in reference [17] and applications of modal space control for active wave suppression were studied in references [12, 18]. In a series of papers [19–21], Tanaka and Kikushima developed the active sink method to suppress all the modes of a flexible beam. Other pertinent papers include a theoretical and experimental work on the wave-absorbing control of a hanging beam [22], and the power flow and strength requirements of active wave control of a flexible beam [23].

The translation motion of a string makes it a gyroscopic system, and one consequence is that the modes do not constitute a standing wave pattern. The modes are non-symmetrical and propagating waves have spatially dependent phases. This gyroscopic property thus renders the construction of observers difficult. To avoid the spillover instability, Yang and Mote proposed a new approach for the active control of the translating string by a distributed transfer function formulation [24]. Time delay and velocity feedback type of controllers were developed [25–27]. Ulsoy examined the vibration control of gyroscopic systems by a pole allocation method [28]. Boundary control by a Lyapunov-type analysis was investigated for both the linear and non-linear moving strings [29–33]. It was shown that the non-linear string can be stabilized by a linear velocity feedback control at a boundary [32, 33]. The vibration suppression of a non-linear travelling string by a variable structure control was examined in reference [34].

Application of wave cancellation to the vibration control of an axially moving string was first considered by Chung and Tan [35]. The idea is to apply a boundary control force such that this boundary appears to be infinite (no wave is reflected). It was shown that all vibration modes can be stabilized and that the controlled string has no resonance. The proposed controller consists of a velocity sensor, a proportional gain and a time delay, and is effective and fairly robust for both unconstrained and constrained string systems. However, practical issues limit the applicability of boundary control for axially moving systems. To circumvent this limitation, a space feedforward control of the travelling waves was proposed [36]. With this controller, vibration in the region downstream of the control force can be cancelled.

Despite the usefulness of the wave absorption concept, two issues remain unsolved before it can be applied to practical situations of axially moving systems. First, the fixed–fixed boundary of reference [36] is an idealization which decouples the translating string spans. Measurement errors, model uncertainties, and even time-varying conditions require that a general boundary condition model to be included in the control problem. Second, the stability of this type of feedforward control must be improved. The purpose of this paper is to develop an active wave control scheme for the axially moving string, with emphasis to resolve these two issues. Verifications of the theoretical predictions are provided by experiments on belt drive and chain drive systems. This manuscript is organized as follows. The control model is given in section 2 and the wave dynamics of the uncontrolled string is summarized in section 3. Design and stability of the active wave controller are discussed in sections 4 and 5, followed by experimental verifications in section 6.

2. PROBLEM FORMULATION

Figure 1 shows an axially moving string of uniform density ρ and under constant tension P, travelling at a constant transport velocity V between two arbitrary boundaries separated by a distance L. The string is excited transversely by an external force $F(X, T)$. The following non-dimensional variables are introduced:

$$x = \frac{X}{L}, \quad w = \frac{W}{L}, \quad f = \frac{FL}{P}, \quad t = T\left(\frac{P}{\rho L^2}\right)^{1/2}, \quad c = V\left(\frac{\rho}{P}\right)^{1/2}. \tag{1}$$

Applying the Hamilton's Principle, the normalized equation of motion governing the transverse displacement $w(x, t)$ of the translating string is [1]

$$w_{,tt}(x, t) + 2cw_{,xt}(x, t) - (1 - c^2)w_{,xx}(x, t) = f(x, t) + q_1(x, t) + q_2(x, t), \; x \in (0, 1), \; t \geqslant 0, \tag{2}$$

where $(\cdot)_{,t}$ denotes $\partial(\cdot)/\partial t$, $(\cdot)_{,x}$ denotes $\partial(\cdot)/\partial x$, and the control forces are

$$q_1(x, t) = \delta(x - a_1)q_{a1}(t), \qquad q_2(x, t) = \delta(x - a_2)q_{a2}(t). \tag{3}$$

Define the region to the right (left) of an applied force as downstream (upstream). The control objective is to design control laws for the point actuator forces $q_1(x, t)$ and $q_2(x, t)$ such that the vibrations in the upstream and downstream regions of the control forces are cancelled. Initial conditions for the string are specified as

$$w(x, t)|_{t=0} = u_0(x), \qquad w_{,t}(x, t)|_{t=0} = v_0(x), \qquad x \in (0, 1) \tag{4}$$

and the boundary conditions are

$$Mw(x, t)|_{x=0} = \gamma_{B0}(t), \qquad Nw(x, t)|_{x=1} = \gamma_{B1}(t), \qquad t \geqslant 0. \tag{5}$$

In the above equation, M and N are second order temporal-spatial, linear differential operators. A critical speed $c_{cr} = 1$ exists at which all natural frequencies of the uncontrolled string vanish and a buckling type of instability occurs [2]. In the present study, assume $c < 1$.

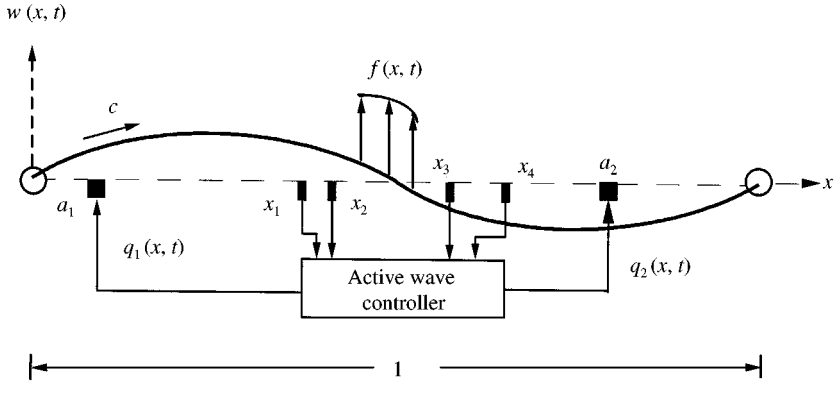

Figure 1. Schematic diagram of an axially moving string with active wave control.

3. WAVE DYNAMICS OF THE UNCONTROLLED STRING

In order to derive the control laws, the wave dynamics of the uncontrolled axially moving string (i.e., $q_i(x, t) = 0$) is briefly described here; see details in reference [37]. Introduce the change of variables

$$\zeta = x - (1 + c)t, \qquad \eta = x + (1 - c)t. \tag{6}$$

The homogeneous "wave equation" (2) then becomes

$$\frac{\partial^2 w(\zeta, \eta)}{\partial \zeta \, \partial \eta} = 0, \tag{7}$$

which states that the solution of equation (7) consists of disturbances propagating to the right at speed $1 + c$ and to the left at speed $1 - c$. These are the forward and backward propagating waves respectively. The response and spectrum of the string are determined from the system transfer functions [38]. Accordingly, the Laplace transform of equations (2), (4) and (5) with respect to t gives

$$s^2 \bar{w}(x, s) + 2cs \frac{\partial}{\partial x} \bar{w}(x, 2) - (1 - c^2) \frac{\partial^2}{\partial x^2} \bar{w}(x\, s) = \bar{f}_e(x, s), \tag{8a}$$

$$\bar{f}_e(x, s) \equiv \bar{f}(x, s) + s u_0(x) + v_0(x) + 2c \frac{\partial}{\partial x} u_0(x), \tag{8b}$$

$$\bar{M}\bar{w}(x, s)|_{x=0} = A_0(s)\bar{w}(0, s) + B_0(s)\bar{w}_{,x}(0, s) = \bar{\gamma}_{B0} + \bar{\gamma}_{I0} \equiv \bar{\gamma}_{t0}(s), \tag{8c}$$

$$\bar{N}\bar{w}(x, s)|_{x=1} = A_1(s)\bar{w}(1, s) + B_1(s)\bar{w}_{,x}(1, s) = \bar{\gamma}_{B1} + \bar{\gamma}_{I1} \equiv \bar{\gamma}_{t1}(s), \tag{8d}$$

where s is the complex Laplace transform variable, $\bar{w}(\cdot, s), \bar{f}(\cdot, s)$ and $\bar{\gamma}_{Bj}(s)$ are the Laplace transform of $w(\cdot, t)$, $f(\cdot, t)$ and $\gamma_{Bj}(t)$, respectively, and $\bar{\gamma}_{Ij}(s)$ is a polynomial of s representing the initial conditions at the boundaries $x = 0, 1$. Henceforth, the index $j = 0, 1$ is used to denote the left and right boundaries respectively. $\bar{M}$ and $\bar{N}$ are the operators M and N with their time derivative operators $\partial/\partial t$ and $\partial^2/\partial t^2$ replaced by s and s^2 respectively.

From equations (6) and (7), the basic wave motion is of the form $e^{(st + \lambda x)}$ where λ is a complex wave number. From equation (8a), the characteristic roots of the homogeneous equation

$$\lambda_1 = \frac{s}{1 - c}, \qquad \lambda_2 = \frac{-s}{1 + c} \tag{9}$$

are the wave numbers of the backward and forward propagating waves respectively. The exact response solution to equations (8a–d) is

$$\bar{w}(x, s) = \int_0^1 G(x, \xi, s) \bar{f}_e(\xi, s) \, d\xi + \sum_{j=0}^{1} h_j(x, s) \bar{\gamma}_j(s), \tag{10}$$

where the closed-form transfer function $G(x, \xi, s)$ and the boundary influence functions $h_j(x, s)$ of the translating string can be evaluated explicitly [38]:

$$G(x,\xi,s)=\begin{cases}\dfrac{e^{\lambda_2(x-\xi)}+\theta_0(s)e^{\lambda_2 x-\lambda_1\xi}+\theta_0(s)\theta_1(s)e^{\lambda_2-\lambda_1(1+\xi-x)}+\theta_1(s)e^{\lambda_2(1-\xi)-\lambda_1(1-x)}}{2s(1-\theta_0(s)\theta_1(s)e^{\lambda_2-\lambda_1})} & x\geqslant\xi,\\ \dfrac{e^{-\lambda_1(\xi-x)}+\theta_0(s)e^{\lambda_2 x-\lambda_1\xi}+\theta_0(s)\theta_1(s)e^{\lambda_2(1+x-\xi)-\lambda_1}+\theta_1(s)e^{\lambda_2(1-\xi)-\lambda_1(1-x)}}{2s(1-\theta_0(s)\theta_1(s)e^{\lambda_2-\lambda_1})} & x\leqslant\xi,\end{cases} \tag{11a}$$

$$h_0(x,s)=\frac{e^{\lambda_2 s}+\theta_1(s)e^{\lambda_2-\lambda_1(1-x)}}{1-\theta_0(s)\theta_1(s)e^{\lambda_2-\lambda_1}},\qquad h_1(x,s)=\frac{e^{-\lambda_1(1-x)}+\theta_0(s)e^{\lambda_2 x-\lambda_1}}{1-\theta_0(s)\theta_1(s)e^{\lambda_2-\lambda_1}}. \tag{11b, c}$$

By equations (10) and (11b, c), the excitations $\bar{\gamma}_j(s)$ are

$$\bar{\gamma}_0(s)=\frac{\bar{\gamma}_{t0}(s)}{A_0(s)+\lambda_2 B_0(s)},\qquad \bar{\gamma}_1(s)=\frac{\bar{\gamma}_{t1}(s)}{A_1(s)+\lambda_1 B_1(s)}, \tag{12}$$

In equations (11a–c), the complex boundary coefficient functions are

$$\theta_0(s)=\frac{1+(1+c)sZ_0(s)}{1-(1-c)sZ_0(s)},\qquad \theta_1(s)=-\frac{1+(1-c)sZ_1(s)}{1-(1+c)sZ_1(s)}, \tag{13}$$

where the complex compliance functions (displacement/force) $Z_j(s)$ are defined as [39]

$$Z_0(s)=\frac{-\bar{w}(0,s)}{(1-c^2)\bar{w}_{,x}(0,s)},\qquad Z_1(s)=\frac{\bar{w}(1,s)}{(1-c^2)\bar{w}_{,x}(1,s)}. \tag{14}$$

In general, string spans are decoupled only for the case of fixed–fixed boundary condition. To derive $\theta_0(s)$, it is assumed that material particles arrive at $x=0$ from $-\infty$ and that waves are transmitted through this boundary to $-\infty$. A similar assumption applies to the boundary at $x=1$. Consider an example of boundary with a dashpot. It can be shown that $Z_0(s)=-1/[s(1+c)+s\beta_0]$, where β_0 is a damping constant. From equations (13), $\theta_0(s)=-\beta_0/(2+\beta_0)$ which is as expected the reflection coefficient [40, 41]. Hence, depending on the modelling assumptions, the effects of general boundary conditions on the string response can be conveniently described by $\theta_j(s)$.

It should be noted that the exponential functions in equations (11a–c) represent delay functions in the time domain. For example, $e^{\lambda_2(x-\xi)}$ is associated with a forward propagating wave travelling from ξ (where the disturbance is applied) to x (where the response is measured). From equation (11a), the system eigenvalues are determined from the characteristic equation

$$1-\theta_0(s)\theta_1(s)e^{\lambda_2-\lambda_1}=0. \tag{15}$$

Based on equations (11a–c), the response solution (10) can be expressed as

$$\bar{w}(x,s)=\theta_0(s)\theta_1(s)e^{\lambda_2-\lambda_1}\bar{w}(x,s)+\int_0^x[G_D^+(x,\xi,s)+G_D^-(x,\xi,s)]\bar{f}_e(\xi,s)\,d\xi$$
$$\times\int_x^1[G_U^+(x,\xi,s)+G_U^-(x,\xi,s)]\bar{f}_e(\xi,s)\,d\xi+\sum_{j=0}^{1}[H_j^+(x,s)+H_j^-(x,s)]\bar{\gamma}_j(s), \tag{16}$$

where the propagation functions are listed in Appendix A, and their physical meanings are given in reference [37]. In equation (16), subscripts D and U denote the downstream and upstream positions respectively, while superscripts $+$ and $-$ denote the forward and backward directions of wave propagation respectively. The G propagation functions are unit impulse response functions. For example, in response to an applied impulse, $G_D^+(x, \xi, s)$ represents the propagation of the forward wave in the downstream region. In view of equation (16), the response consists of a resident wave (the first term) and propagating waves due to external excitations, initial conditions and boundary conditions. The resident wave involves both $\theta_0(s)$ and $\theta_1(s)$ and a total time delay $t_{td} = 1/(1+c) + 1/(1-c)$, the time required for a wave to propagate from the location x, reflected by both boundaries (separated by a distance $\ell = 1$), and back to x.

4. DESIGN OF ACTIVE WAVE CONTROLLER

Applying the concept of convolution to equation (16) and from earlier results [35], it is seen that the design of controllers is independent of the type of excitation. Thus, in Figure 1, consider a point load applied at $x = d$:

$$\bar{f}(x, s) = \delta(x - d)\bar{f}_d(s). \tag{17}$$

The Laplace transform of the control forces (3) gives

$$\bar{q}_1(x, s) = \delta(x - a_1)\bar{q}_{a1}(s), \quad a_1 < d < a_2, \tag{18}$$

$$\bar{q}_2(x, s) = \delta(x - a_2)\bar{q}_{a2}(s), \quad a_1 < d < a_2, \tag{19}$$

The objective of the active vibration control is to cancel the vibration of the moving string in the regions $x \leqslant a_1$ and $x \geqslant a_2$. For zero initial conditions, the response of the string is

for $0 \leqslant x \leqslant a_1$:

$$\bar{w}(x, s) = \theta_0(s)\theta_1(s)e^{\lambda_2 - \lambda_1}\bar{w}(x, s) + [G_U^+(x, d, s) + G_U^-(x, d, s)]\bar{f}_d(s) + [G_U^+(x, a_1, s) + G_U^-(x, a_1, s)]\bar{q}_{a1}(s) + [G_U^+(x, a_2, s) + G_U^-(x, a_2, s)]\bar{q}_{a2}(s), \tag{20a}$$

for $a_1 \leqslant x \leqslant d$:

$$\bar{w}(x, s) = \theta_0(s)\theta_1(s)e^{\lambda_2 - \lambda_1}\bar{w}(x, s) + [G_U^+(x, d, s) + G_U^-(x, d, s)]\bar{f}_d(s) + [G_D^+(x, a_1, s) + G_D^-(x, a_1, s)]\bar{q}_{a1}(s) + [G_U^+(x, a_2, s) + G_U^-(x, a_2, s)]\bar{q}_{a2}(s), \tag{20b}$$

for $d \leqslant x \leqslant a_2$:

$$\bar{w}(x, s) = \theta_0(s)\theta_1(s)e^{\lambda_2 - \lambda_1}\bar{w}(x, s) + [G_D^+(x, d, s) + G_D^-(x, d, s)]\bar{f}_d(s) + [G_D^+(x, a_1, s) + G_D^-(x, a_1, s)]\bar{q}_{a1}(s) + [G_U^+(x, a_2, s) + G_U^-(x, a_2, s)]\bar{q}_{a2}(s), \tag{20c}$$

for $a_2 \leqslant x \leqslant 1$:

$$\bar{w}(x, s) = \theta_0(s)\theta_1(s)e^{\lambda_2 - \lambda_1}\bar{w}(x, s) + [G_D^+(x, d, s) + G_D^-(x, d, s)]\bar{f}_d(s) + [G_D^+(x, a_1, s) + G_D^-(x, a_1, s)]\bar{q}_{a1}(s) + [G_D^+(x, a_2, s) + G_D^-(x, a_2, s)]\bar{q}_{a2}(s). \tag{20d}$$

It is realized that no wave can propagate in $x \leqslant a_1$ ($x \geqslant a_2$) if all backward (forward) propagating waves in this region are conceled by $\bar{q}_{a1}(s)$ ($\bar{q}_{a2}(s)$). Based on this idea and from equations (20a, d), the following control laws are proposed:

$$G_U^-(x, a_1, s)\bar{q}_{a1}(s) = -G_U^-(x, d, s)\bar{f}_d(s) - G_U^-(x, a_2, s)\bar{q}_{a2}(s), \tag{21}$$

$$G_D^+(x, a_2, s)\bar{q}_{a2}(s) = -G_D^+(x, d, s)\bar{f}_d(s) - G_D^+(x, a_1, s)\bar{q}_{a1}(s). \tag{22}$$

Simplifying equations (21) and (22) leads to explicit expressions of the control forces in terms of $\bar{f}_d(s)$:

$$\bar{q}_{a1}(s) = \frac{e^{\lambda_2(a_2-d)-\lambda_1(a_2-a_1)} - e^{-\lambda_1(d-a_1)}}{1 - e^{(\lambda_2-\lambda_1)(a_2-a_1)}}\bar{f}_d(s), \tag{23}$$

$$\bar{q}_{a2}(s) = \frac{e^{\lambda_2(a_2-a_1)-\lambda_1(d-a_1)} - e^{\lambda_2(a_2-d)}}{1 - e^{(\lambda_2-\lambda_1)(a_2-a_1)}}\bar{f}_d(s), \tag{24}$$

Substituting the above results into equations (20a–d) gives the response solution of the controlled axially moving string with zero initial conditions:

$$\bar{w}(x, s) =$$

$$\begin{cases} 0, & 0 \leqslant x \leqslant a_1, \\ \dfrac{e^{-\lambda_1(d-x)} - e^{\lambda_2(x-a_1)-\lambda_1(d-a_1)} + e^{\lambda_2(a_2+x-d-a_1)-\lambda_1(a_2-a_1)} - e^{\lambda_2(a_2-d)-\lambda_1(a_2-x)}}{2s(1 - e^{(\lambda_2-\lambda_1)(a_2-a_1)})}\bar{f}_d(s), & a_1 \leqslant x \leqslant d, \\ \dfrac{e^{\lambda_2(x-d)} - e^{\lambda_2(x-a_1)-\lambda_1(d-a_1)} + e^{\lambda_2(a_2-a_1)-\lambda_1(a_2+d-x-a_1)} - e^{\lambda_2(a_2-d)-\lambda_1(a_2-x)}}{2s(1 - e^{(\lambda_2-\lambda_1)(a_2-a_1)})}\bar{f}_d(s), & d \leqslant x \leqslant a_2, \\ 0, & a_2 \leqslant x \leqslant 1. \end{cases} \tag{25}$$

The above result states that the response of the controlled string in the regions $x \leqslant a_1$ and $x \geqslant a_2$ becomes zero if the uncontrolled string is not at resonance. It was pointed out that, for a fixed–fixed string, the same result was obtained by either imposing a partial wave cancellation (i.e., those of equations (21, 22)) or cancelling both the forward and backward waves (total cancellation) [36]. However, total wave cancellation leads to much more complicated control laws. For the present problem with arbitrary boundary conditions, it can also be shown that total wave cancellation leads to the same result given by equation (25). The response of the controlled string to a distributed excitation force can be expressed in the integral form

$$\bar{w}(x, s) = \int_{a_1}^{a_2} G_c(x, \xi, s)\bar{f}_e(\xi, s)\,d\xi, \tag{26}$$

where the closed-loop transfer function $G_c(x, \xi, s)$ is deduced from equation (25) by replacing d with ξ.

It should be noted that the implementation of the control laws (23) and (24) is not feasible since excitation force signals are difficult to measure. Control forces are generally expressed

in terms of displacement or velocity. It is thus necessary to establish relations between the control forces and displacement measurements. Four sensors are located along the string as shown in Figure 1. As shown in Appendix B, the control forces are derived as

$$\bar{q}_{a1} = -\frac{2s[\bar{w}(x_2, s) - \bar{w}(x_1, s)e^{\lambda_2(x_2 - x_1)}]e^{-\lambda_1(x_2 - a_1)}}{1 - e^{(\lambda_2 - \lambda_1)(x_2 - x_1)}}, \tag{27}$$

$$\bar{q}_{a2} = -\frac{2s[\bar{w}(x_3, s) - \bar{w}(x_4, s)e^{\lambda_2(x_4 - x_3)}]e^{\lambda_2(a_2 - x_3)}}{1 - e^{(\lambda_2 - \lambda_1)(x_4 - x_3)}}. \tag{28}$$

4.1. REMARKS

(1) With the control forces given by equations (27) and (28), the vibration of the translating string in $x \leqslant a_1$ and $x \geqslant a_2$ tends to zero asymptotically (see equation (25)).

(2) Comparing equation (25) with equation (11a), it can be seen that the transfer functions of the uncontrolled and controlled strings are of the same form, but the controlled string has an effective length of $a \equiv a_2 - a_1$. Since $\theta_0(s) = \theta_1(s) = -1$ for the fixed–fixed boundary condition, it is concluded that the control forces effectively act as fixed supports (holders) which limit the vibration of the string within $x \in (a_1, a_2)$ and eliminate any vibration outside of this region. A straightforward derivation shows that $\bar{q}_{a1}(s)$ and $\bar{q}_{a2}(s)$ are indeed equal to the boundary support forces of a fixed–fixed string with length a. It should be noted that, since the boundary conditions of the uncontrolled string are arbitrary, these results hold even when there are uncertainties in the boundary conditions.

Corollary. *Suppose only $q_2(x, t)$ is applied at $x = a_2$ (downstream wave cancellation), then the controlled string is effectively of length a_2 with boundary condition described by $\theta_0(s)$ at $x = 0$ and $\theta_{a2}(s) = -1$ at $x = a_2$. The corresponding $G_c(x, \xi, s)$ and system response can easily be deduced from equation* (11a).

(3) Equations (27) and (28) show that each controller consists of a velocity sensor and time delay of two observers. These control laws are easy to implement.

(4) The controllers are shown to be independent of the location and type of the excitation force, and the boundary conditions of the uncontrolled string.

4.2. NUMERICAL RESULTS

The following non-dimensional parameters are used to obtain the numerical results:

$$c = 0{\cdot}3, \quad x_1 = 0{\cdot}4, \quad x_2 = 0{\cdot}45, \quad x_3 = 0{\cdot}55, \quad x_4 = 0{\cdot}6, \quad d = 0{\cdot}5, \quad a_1 = 0{\cdot}3, \quad a_2 = 0{\cdot}7.$$

A dashpot is placed at each boundary with damping constants $\beta_0 = \beta_1 = 2$. A sinusoidal point load of frequency $\omega = 3{\cdot}2\pi$ is applied. All simulation results are obtained by MatLab.

In order to understand the simulation results, it is noted that the control forces (27) and (28) are derived under the assumption of zero initial conditions at the boundaries, i.e., $\bar{\gamma}_j(s) = 0$ in equation (16). However, in practice, control forces may not be applied at the same time when the system is "turned on" (at $t = 0$). Thus, $\bar{\gamma}_j(s)$ may be non-zero at the instant t_c when the control is applied. Hence, for systems with non-fixed boundaries, the controller may not be able to suppress the vibration to zero as the control objective has

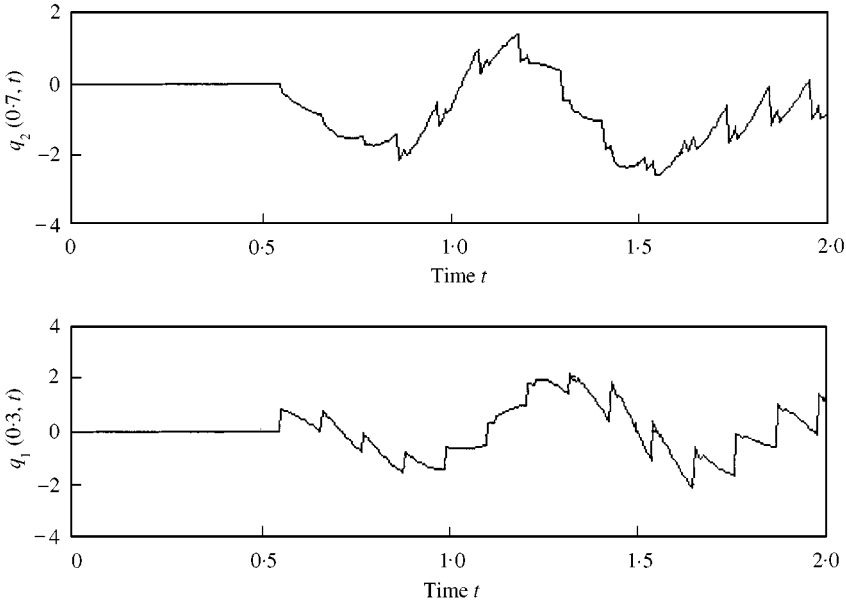

Figure 2. An example of the time history of "real-time" control forces.

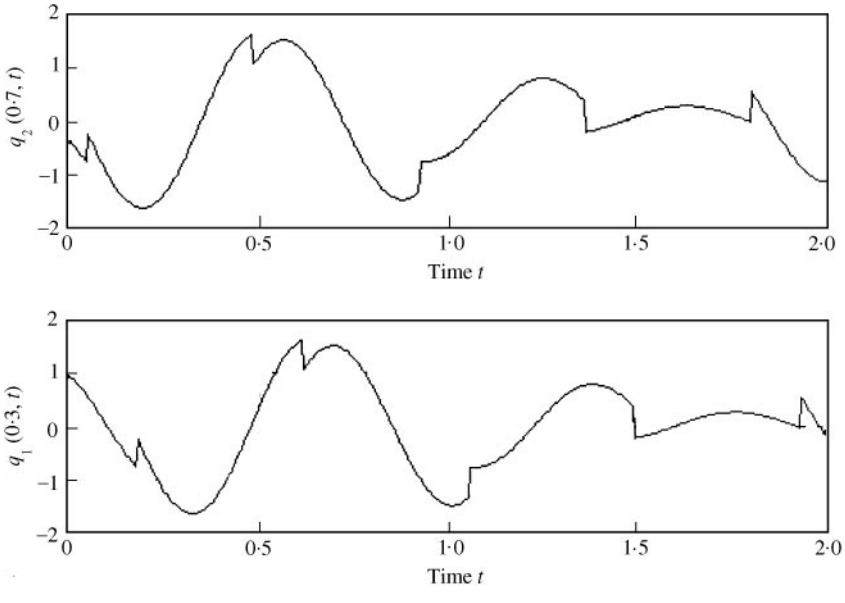

Figure 3. An example of the time history of "simulation" control forces.

stated, even though the initial conditions are zero. The control force which is applied at t_c is defined as "real time", i.e., it is computed without any knowledge of the response history during $0 \leqslant t \leqslant t_c$, and the control force which tracks the response history during $0 \leqslant t \leqslant t_c$ as "simulation". The latter is suitably termed "simulation" because it can be achieved only in simulations but not in real time control.

The "real time" and "simulation" control forces for this example are plotted in Figures 2 and 3. The corresponding responses of the controlled system are shown in Figures 4 and 5.

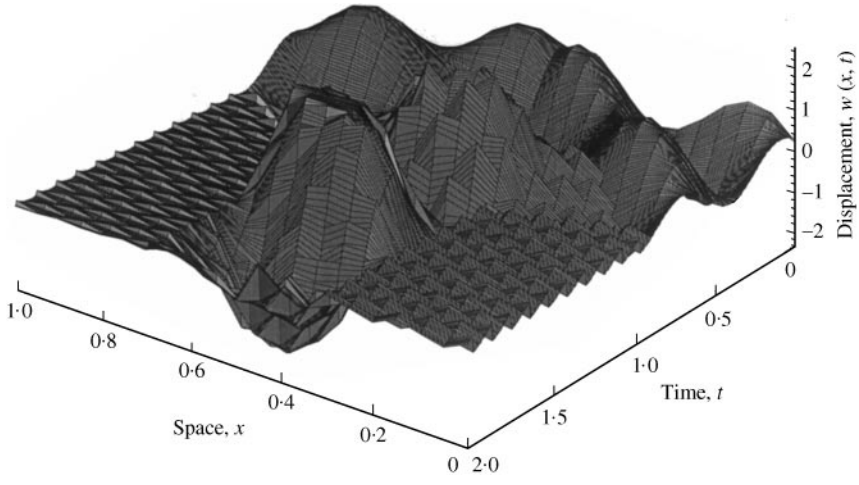

Figure 4. Response of the axially moving string under a sinusoidal point load and controlled by the "real-time" control forces of Figure 2.

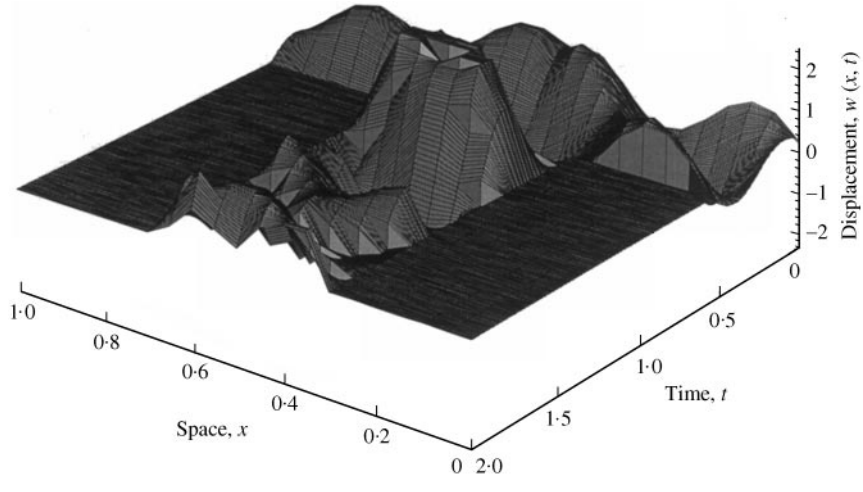

Figure 5. Response of the axially moving string under a sinusoidal point load and controlled by the "simulation" control forces of Figure 3.

In Figure 4, it is seen that the controlled vibration does not go to zero as a result of non-zero motions at the boundaries when the control forces are applied at t_c. However, the controlled amplitude is much smaller than the uncontrolled one. In Figure 5, as predicted by the control laws, the vibration is suppressed to zero in $x \leqslant a_1$ and $x \geqslant a_2$. Comparing Figures 4 and 5, it is seen that the control is still effective in the presence of non-zero initial conditions at non-fixed boundaries. For this type of feedforward control, disturbances in the uncontrolled regions and boundary excitations can be attenuated by feedback control [36]. Numerical results show that similar control effects are obtained when different types of boundary conditions are considered and when a random excitation force is applied.

5. STABILITY OF CONTROLLER

Simulation results have shown that the active wave control is effective for suppressing the vibration in the upstream and downstream regions of the control forces. However, this is based on ideal conditions, and the stability and robustness of the control scheme must be examined. To study the stability of the controlled system, a stability theorem is first stated. A stabilization coefficient is then introduced to improve the robustness of the control. The stability of general linear time-delay systems can be referred to, for example, reference [42], and for the axially moving string, see for example reference [24].

The characteristic equations of both the uncontrolled and controlled systems have the general form of

$$1 - \varphi(s)\mathrm{e}^{-\tau s} = 0, \tag{29}$$

where $\varphi(s)$ is a function related to the boundary conditions and τ is a time delay. It is noted that the denominators of the control forces are also in the form of equation (29).

Theorem. *Consider a system which has a characteristic equation of the form* (29), *where* τ *is positive real. The system is asymptotically stable iff* $|\varphi(s)| < 1$, *marginally stable iff* $|\varphi(s)| = 1$, *and unstable iff* $|\varphi(s)| > 1$.

The proof is given in Appendix C.

From equation (29), it is noted that the stability of the uncontrolled string is affected by the boundary conditions since $\varphi(s) = \theta_0(s)\theta_1(s)$. Consider the fixed–fixed boundary, $\theta_0(s) = \theta_1(s) = -1$. By the theorem, the string is marginally stable because $|\varphi(s)| = 1$. Thus, the control forces (27) and (28) are also marginally stable. This means that the proposed active vibration control scheme is not robust enough to perform a stable control in real time under a noisy environment of practical test conditions. This is typical of a feedforward control [11]. Figure 6 shows the time response of the controlled axially moving string when there is a 5% white noise in the amplitude of the excitation force applied at $x = 0{\cdot}05$. Only one control force $q_2(x, t)$ is applied at $a_2 = 0{\cdot}5$. It is seen that the downstream vibration does not go to zero, but is bounded. However, the control force, shown in Figure 7, appears

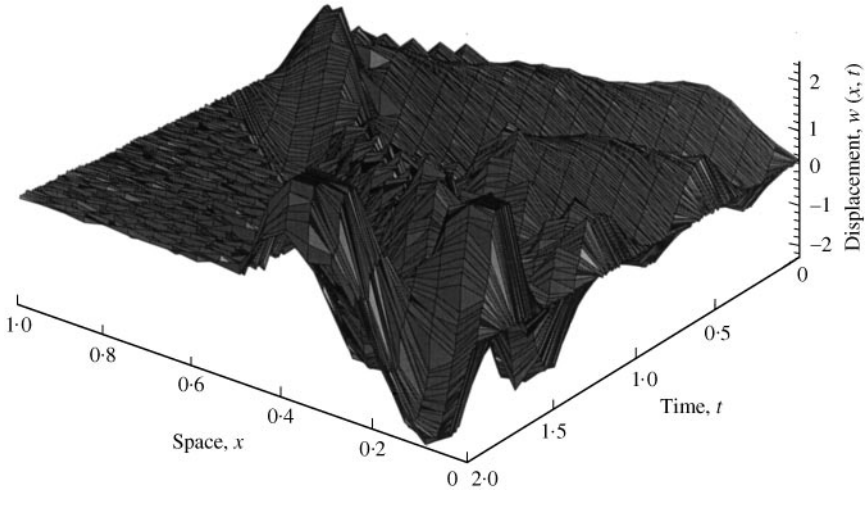

Figure 6. Response of the controlled axially moving string with 5% white noise in the amplitude of the sinusoidal excitation. Control force $q_{a1}(x, t) = 0$; $c = 0{\cdot}3$, $d = 0{\cdot}05$, $x_3 = 0{\cdot}25$, $x_4 = 0{\cdot}3$, $a_2 = 0{\cdot}5$.

to increase unboundedly with time. It is thus necessary to resolve the robustness issue of the controllers before they can be applied for real-time control. Based on the stability theorem, stabilization coefficients $s_{c1} < 1$ and $s_{c2} < 1$ are introduced to the control forces (27) and (28) in order to improve their stability. The modified control forces become

$$\bar{q}_{a1}(s) = -\frac{2s[\bar{w}(x_2, s) - \bar{w}(x_1, s)e^{\lambda_2(x_2 - x_1)}]e^{-\lambda_1(x_2 - a_1)}}{1 - s_{c1}e^{(\lambda_2 - \lambda_1)(x_2 - x_1)}}, \tag{30}$$

$$\bar{q}_{a2}(s) = -\frac{2s[\bar{w}(x_3, s) - \bar{w}(x_4, s)e^{-\lambda_1(x_4 - x_3)}]e^{\lambda_2(a_2 - x_3)}}{1 - s_{c2}e^{(\lambda_2 - \lambda_1)(x_4 - x_3)}}. \tag{31}$$

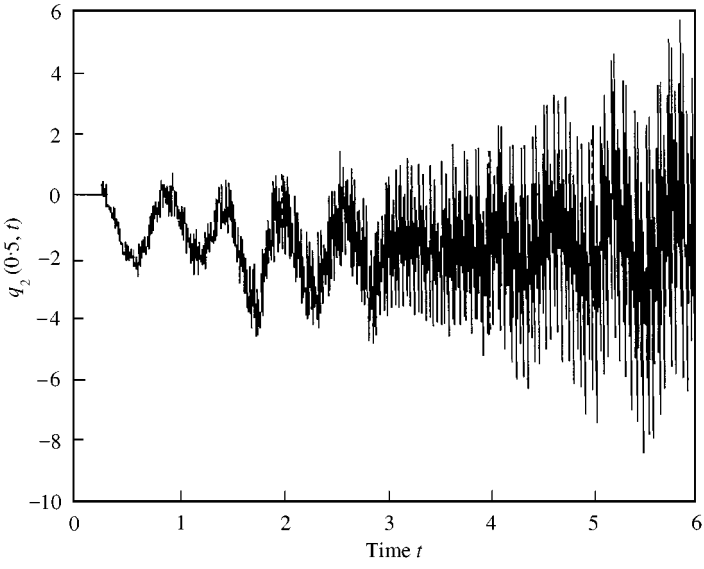

Figure 7. Time history of the control force when the excitation force has 5% noise, $s_{c2} = 1$ (no stabilization effect).

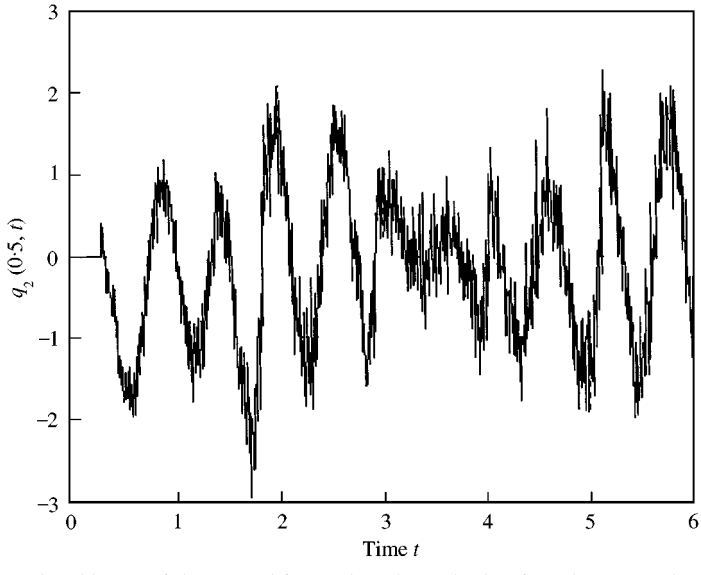

Figure 8. Time history of the control force when the excitation force has 5% noise, $s_{c2} = 0{\cdot}8$.

Note that equations (30) and (31) are obtained without changing the basic structure of the control law. The stabilization coefficients effectively add damping to the system. A smaller coefficient improves the robustness but reduces the performance of the controller. From the experiments (see section 6), compromised values of the stabilization coefficients are found to be between 0·8 and 0·9. Figure 8 plots the control force $q_{a2}(0{\cdot}5, t)$ with $s_{c2} = 0{\cdot}8$, based on 5% noise in the excitation force. It is noted that the control signal is now bounded.

6. EXPERIMENTAL SET-UP AND RESULTS

A schematic of the active vibration control system is depicted in Figure 9. Experiments were conducted on metallic belt drive and automotive engine chain drive systems. A photograph of the experimental set-up of sensors and actuators for the belt drive system is shown in Figure 10. The driving pulley/sprocket is driven directly by a DC motor with an adjustable speed range up to 1750 r.p.m. The test stand allows experiments to be conducted on belts/chains of different lengths and under different tensions (note the tension adjustment mechanism in Figure 9). On-line data processing and active control are processed by a high-performance DSP board (TMS320C30). Figure 10 shows the set-up for downstream wave cancellation experiments. Displacements are observed by non-contact sensors (Model Electro 85003) located at X_3 and X_4, and another displacement signal is measured downstream at X_5 for the comparison of uncontrolled and controlled amplitudes. Excitation and controller actuation are provided by magnetic pickups (Model 3040H20) with a maximum response frequency of 40 kHz. The function of these pickups (sensors) become actuation when the reverse principle of electromagnetism is applied.

The vibration control experiments were conducted with only $q_{a2}(x, t)$. First, the effect of the stabilization coefficient and the correctness of the real-time control programming were verified. Control signals were generated and tested by feeding two sinusoidal signals of 50 Hz with 5% noise (these signals simulate the observer measurements) into the active

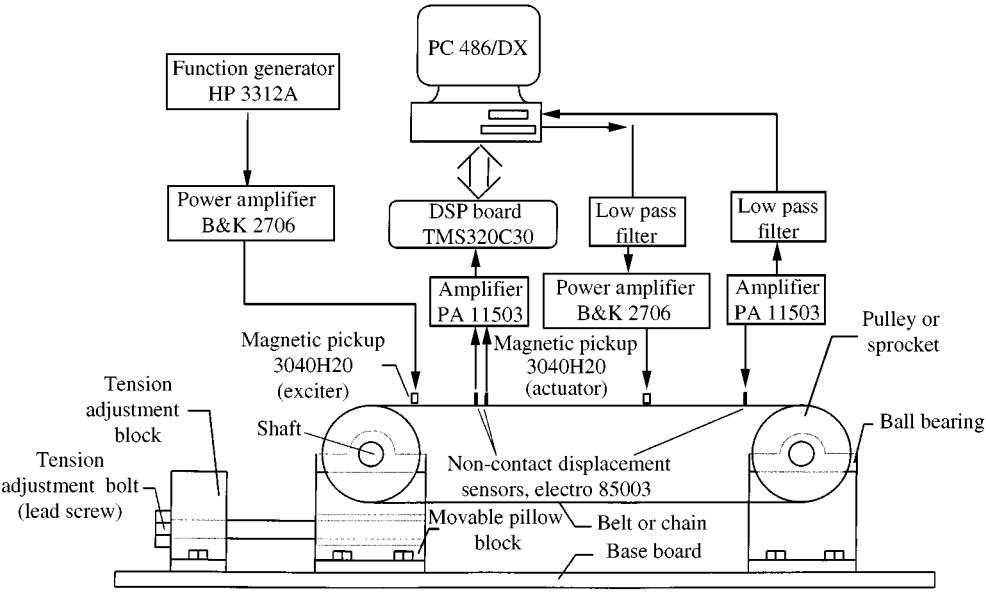

Figure 9. A schematic diagram of the experimental active vibration control system.

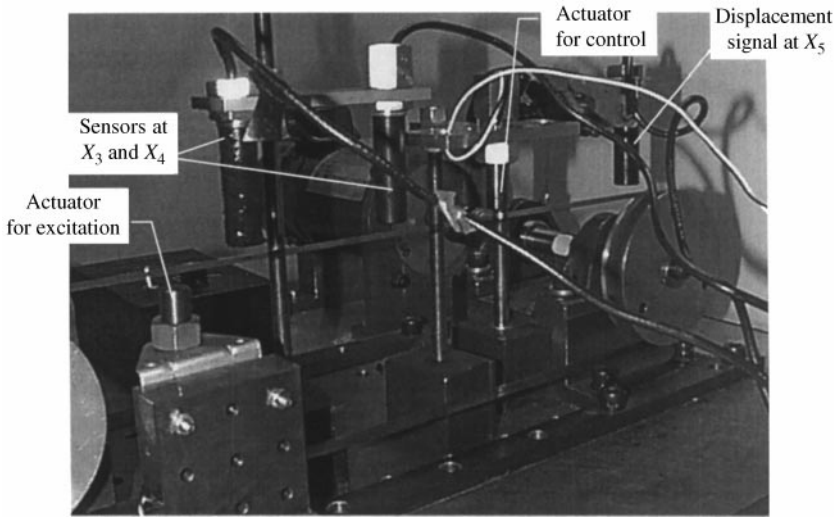

Figure 10. Experimental set-up of sensors and actuators for a belt drive system.

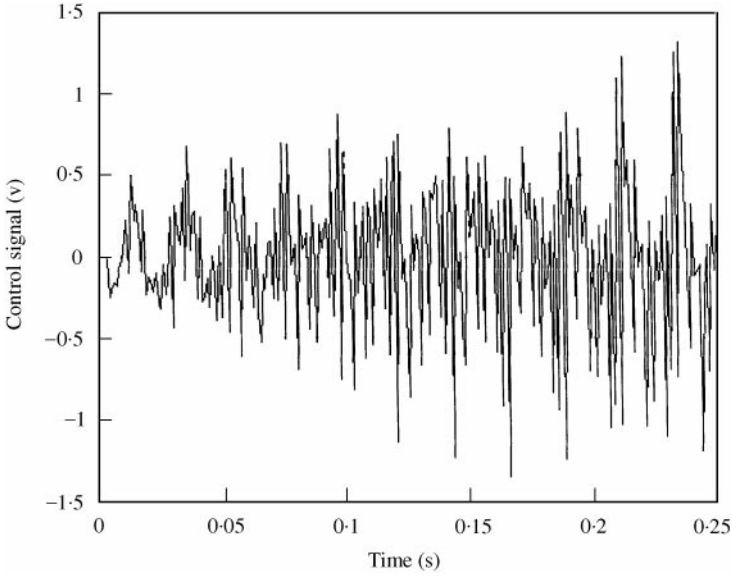

Figure 11. Time history of the control force signal with 5% noise in the input signals, $s_{c2} = 1$ (no stabilization effect).

wave controller. Figure 11 shows that the amplitude of the control signal increases with time and is unstable. In Figure 12, a stabilization coefficient $s_{c2} = 0{\cdot}9$ is applied and the signal becomes stable, demonstrating the improved stability and robustness of the controller. This stabilization effect agrees well with the theoretical prediction discussed in the previous section.

Experiments were performed on different sets of operating parameters. All results showed that the controller was effective. Two cases are reported here with parameters listed in Table 1. The belt vibration was measured in the speed range of 0–350 r.p.m. with 25 r.p.m.

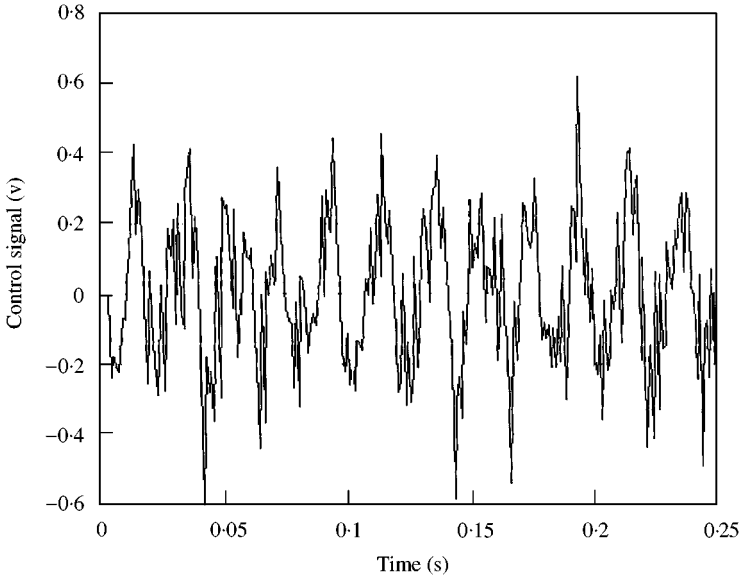

Figure 12. Time history of the control force signal with 5% noise in the input signals, $s_{c2} = 0{\cdot}9$.

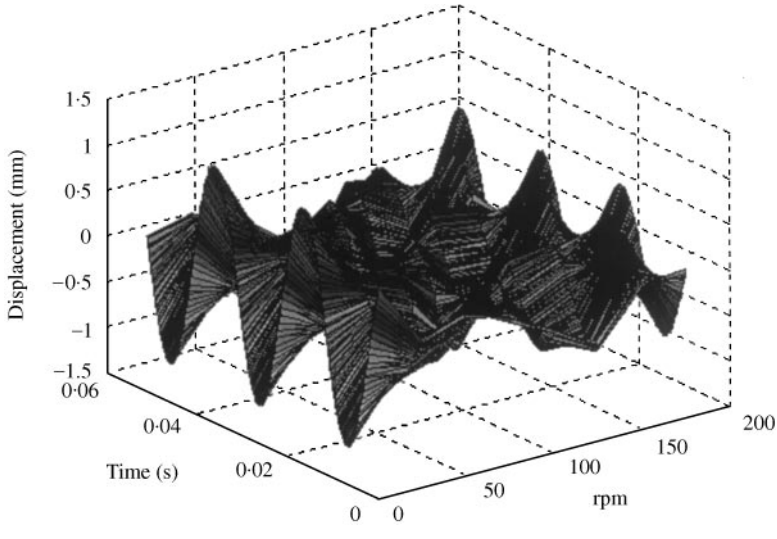

Figure 13. Time history of the uncontrolled belt vibration as a function of speed. The belt tension is 99 N, span length is 0·576 m and displacement is measured at 0·41 m.

TABLE 1

List of experimental parameters

	Tension (N)	Span length (m)	X_3 (m)	X_4 (m)	A_2 (m)	X_5 (m)
Belt	99·0	0·576	0·146	0·241	0·276	0·410
Chain	235·1	0·400	0·064	0·159	0·203	0·330

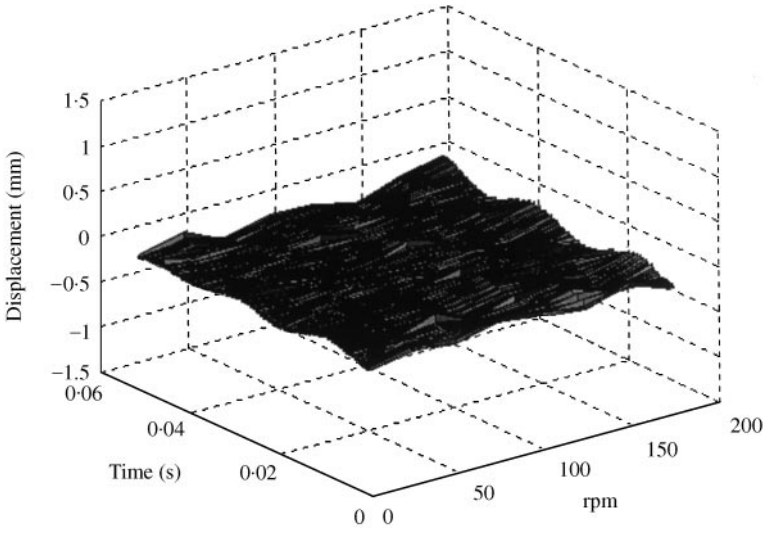

Figure 14. Time history of the controlled belt vibration as a function of speed. The belt tension is 99 N, span length is 0·576 m and displacement is measured at 0·41 m.

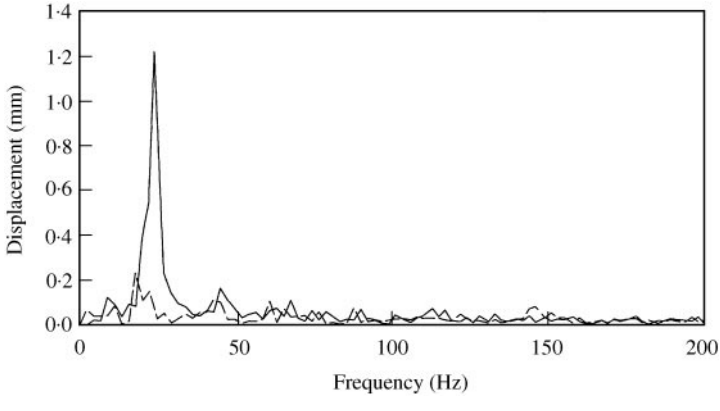

Figure 15. Frequency response of the uncontrolled (– – –) and controlled (——) chain vibrations at 1160 r.p.m. The chain tension is 235·1 N, span length is 0·4 m and displacement is measured at 0·33 m.

increment. The pulley diameter is 0·11 m and the transport velocity V thus varies from 0–2·02 m/s. Figures 13 and 14 (plotted on the same scale) compare the time histories of the uncontrolled and controlled belt vibrations as a function of the pulley speed. The active control reduces the vibration amplitude by 80–95% throughout this speed range. Other results for different belt tensions show that there is at least 70% reduction in the vibration amplitude.

The chain vibration was measured in the speed range of 0–1750 r.p.m. with 87·5 r.p.m. increment. The sprocket diameter is 0·12 m and the transport velocity V thus varies from 0–11 m/s. The fundamental natural frequency reduced from 22 Hz (at zero r.p.m.) to about 13·3 Hz (at 1750 r.p.m.). In Figure 15, the frequency responses of the uncontrolled and controlled vibration at 1160 r.p.m. are plotted. It is seen that the active control suppresses the amplitude of the resonant mode by at least 80%.

7. SUMMARY AND CONCLUSIONS

An active vibration control scheme based on wave cancellation is developed for an axially moving string with general boundary conditions. Two control forces are applied to eliminate the vibration in the upstream and downstream regions. It is shown that the control forces effectively act as fixed supports and are independent of the boundary conditions. Each controller consists of a velocity sensor and time delay of two observers. Although initial conditions are assumed to be zero at the non-fixed boundaries, simulation results show that the controller is still effective. The active wave controller is shown to be marginally stable. Its stability and robustness are improved by introducing a stabilization coefficient in the control forces without changing the structure of the control law. These improvements are verified by both simulations and experiments. The effectiveness of the controller with stabilization coefficient is experimentally demonstrated on both a moving belt drive and an automotive engine chain drive systems.

ACKNOWLEDGMENT

The authors gratefully acknowledge the support of the National Science Foundation, General Motors Corporation, and the Institute for Manufacturing Research at Wayne State University for this research work. The generous assistance of Dr Dishan Huang in the experiments is greatly appreciated.

REFERENCES

1. F. R. ARCHIBALD and A. G. EMSLIE 1958 *ASME Journal of Applied Mechanics* **25**, 347–348. The vibration of a string having a uniform motion along its length.
2. C. D. MOTE JR 1965 *Journal of the Franklin Institute* **279**, 430–444, A study of band saw vibrations.
3. K. W. WANG and S. P. LIU 1991 *Shock and Vibration Digest* **23**, 8–13. On the noise and vibration of chain drive systems.
4. C. C. LIN and C. D. MOTE JR 1995 *ASME Journal of Applied Mechanics* **62**, 772–779. Equilibrium displacement and stress distribution in a two-dimensional axially moving web under transverse loading.
5. W. H. LIAO and K. W. WANG 1997 *ASME Journal of Vibration and Acoustics* **119**, 563–572. On the active-passive hybrid control actions of active constrained layers.
6. M. J. BALAS 1978 *IEEE Automatic Control* **23**, 673–679. Feedback control of flexible system.
7. L. MEIROVITCH and H. BARUH 1982 *AIAA Journal of Guidance, Control, and Dynamics* **5**, 60–66. Control of self-adjoint distributed-parameter systems.
8. C. R. FULLER, S. J. ELLIOTT and P. A. NELSON 1996 *Active Control of Vibration*. London: Academic Press.
9. J. LU, M. J. CROCKER and P. K. RAJU *Journal of Sound and Vibration* **134**, 364–368. Active vibration control using wave control concepts.
10. B. R. MACE 1987 *Journal of Sound and Vibration* **114**, 253–270. Active control of flexural vibrations.
11. R. J. NAGEM and J. H. WILLIAMS JR 1990 *Mechanics of Structures and Machines* **18**, 33–57. Control of a one-dimensional distributed structure based on wave propagation analysis.
12. C.-S. CHOU 1998 *Series on Stability, Vibration and Control of Systems, Series B* (H.-S. Tzou, A. Guran, U. Gabbert, J. Tani and E. Breitbach, editors), vol. 4 (Part II), 133–178. Singapore: World Scientific Publishing Company. Active vibration sink for flexible structures.
13. H. FUJII, T. OHTSUKA and T. MURAYAMA 1992 *AIAA Journal of Guidance, Control, and Dynamics* **15**, 431–439. Wave-absorbing control of flexible structure with non-collocated sensors and actuators.
14. H. FUJII and T. OHTSUKA 1992 *AIAA Journal of Guidance, Control, and Dynamics* **15**, 741–745. Experiment of a noncollocated controller for wave cancellation.

15. H. F. OLSON and E. G. MAY 1953 *Journal of the Acoustical Society of America* **25**, 1130–1136. Electronic sound absorber.
16. M. O. TOKHI and R. R. LEITCH 1992 *Active Noise Control*. Oxford: Oxford University Press.
17. A. H. VON FLOTOW 1986 *AIAA Journal of Guidance, Control, and Dynamics* **9**, 462–468. Travelling wave control for large spacecraft structures.
18. J. K. BENNIGHOF and L. MEIROVITCH 1989 *AIAA Journal of Guidance, Control, and Dynamics* **12**, 555–567. Active suppression of traveling waves in structures.
19. N. TANAKA and Y. KIKUSHIMA 1991 *JSME International Journal Series III* **34**, 159–167. Active wave control of a flexible beam (proposition of the active sink method).
20. N. TANAKA and Y. KIKUSHIMA 1992 *JSME International Journal Series III* **35**, 236–244. Active wave control of a flexible beam (fundamental characteristics of an active sink system and its verification).
21. N. TANAKA and Y. KIKUSHIMA 1999 *ASME Journal of Vibration and Acoustics* **121**, 174–182. Optimal vibration feedback control of an Euler–Bernoulli beam: toward realization of the active sink method.
22. A. H. VON FLOTOW and B. SCHÄFER 1986 *AIAA Journal of Guidance, Control, and Dynamics* **9**, 673–680. Wave-absorbing controllers for a flexible beam.
23. M. J. BRENNAN, S. J. ELLIOTT and R. J. PININGTON 1995 *Journal of Sound and Vibration* **184**, 657–688. Strategies for the active vibration control of flexural vibration on a beam.
24. B. YANG and C. D. MOTE JR 1991 *ASME Journal of Applied Mechanics* **58**, 189–196. Active vibration control of the axially moving string in the *s*-domain.
25. B. YANG and C. D. MOTE JR 1992 *ASME Journal of Dynamic Systems, Measurement, and Control* **114**, 409–415. On time delay in noncollocated control of flexible mechanical systems.
26. B. YANG 1992 *ASME Journal of Dynamic Systems, Measurement, and Control* **114**, 736–740. Noncollocated control of a damped string using time delay.
27. B. YANG 1994 *Journal of Sound and Vibration* **175**, 525–534. Vibration control of gyroscopic systems via direct velocity feedback.
28. A. G. ULSOY 1984 *ASME Journal of Dynamic Systems, Measurement, and Control* **106**, 6–14. Vibration control in rotating or translating elastic systems.
29. C. F. BAICU, C. D. RAHN and B. D. NIBALI 1996 *Journal of Sound and Vibration* **198**, 17–26. Active boundary control of elastic cables.
30. S. JOSHI and C. D. RAHN 1995 *Proceedings of American Control Conference*, 2820–2824. Position control of a flexible cable gantry crane: theory and experiment.
31. S. Y. LEE and C. D. MOTE JR 1996 *ASME Journal of Dynamic Systems, Measurement, and Control* **118**, 66–74. Vibration control of an axially moving string by boundary control.
32. S. M. SHAHRUZ and D. A. KURMAJI 1997 *Journal of Sound and Vibration* **201**, 145–152. Vibration suppression of a non-linear axially moving string by boundary control.
33. S. M. SHAHRUZ 1998 *Automatica* **34**, 1273–1277. Boundary control of the axially moving Kirchhoff string.
34. R.-F. FUNG, J.-S. HUANG, Y.-C. WANG and R.-T. YANG 1998 *International Journal of Mechanical Sciences* **40**, 493–506. Vibration reduction of the nonlinearly traveling string by a modified variable structure control with proportional and integral compensations.
35. C. H. CHUNG and C. A. TAN 1995 *ASME Journal of Vibration and Acoustics* **117**, 49–55. Active vibration control of the axially moving string by wave cancellation.
36. S. YING and C. A. TAN 1996 *ASME Journal of Vibration and Acoustics* **118**, 306–312. Active vibration control of the axially moving string using space feedforward and feedback controllers.
37. C. A. TAN and S. YING 1997 *ASME Journal of Applied Mechanics* **64**, 394–400. Dynamic analysis of the axially moving string based on wave propagation.
38. B. YANG and C. A. TAN 1992 *ASME Journal of Applied Mechanics* **59**, 1009–1014. Transfer functions of one-dimensional distributed parameter systems.
39. P. M. MORSE and K. U. INGARD 1968 *Theoretical Acoustics*. Princeton, NJ: Princeton University Press.
40. S. Y. LEE and C. D. MOTE JR 1997 *Proceedings of the Fifth Pan American Congress of Applied Mechanics–PACAM V, San Juan, Puerto Rico*, Vol. 4, 478–481. Mode localization in a translating medium coupled to stationary constraints.
41. C. H. RIEDEL and C. A. TAN 1998 *Journal of Sound and Vibration* **215**, 455–473. Dynamic characteristics and mode localization of elastically constrained axially moving strings and beams.
42. K. GU 1997 *International Journal of Control* **68**, 923–934. Discretized LMI set in the stability problem of linear uncertain time-delay systems.

APPENDIX A: DEFINITION OF PROPAGATION FUNCTIONS

Referring to equation (16), the propagation functions are

$$G_D^+(x,\xi,s)=\frac{1}{2s}\left[\mathrm{e}^{\lambda_2(x-\xi)}+\theta_0(s)\mathrm{e}^{\lambda_2 x-\lambda_1\xi}\right],\quad x>\xi, \tag{A1}$$

$$G_D^-(x,\xi,s)=\frac{1}{2s}\left[\theta_1(s)\mathrm{e}^{\lambda_2(1-\xi)-\lambda_1(1-x)}+\theta_0(s)\theta_1(s)\mathrm{e}^{\lambda_2-\lambda_1(1+\xi-x)}\right],\quad x>\xi, \tag{A2}$$

$$G_U^+(s,\xi,s)=\frac{1}{2s}\left[\theta_0(s)\mathrm{e}^{\lambda_2 x-\lambda_1\xi}+\theta_0(s)\theta_1(s)\mathrm{e}^{\lambda_2(1+x-\xi)-\lambda_1}\right],\quad x<\xi, \tag{A3}$$

$$G_U^-(x,\xi,s)=\frac{1}{2s}\left[\mathrm{e}^{-\lambda_1(\xi-x)}+\theta_1(s)\mathrm{e}^{\lambda_2(1-\xi)-\lambda_1(1-x)}\right],\quad x<\xi, \tag{A4}$$

$$H_0^+(x,s)=\mathrm{e}^{\lambda_2 x},\qquad H_0^-(x,s)=\theta_1(s)\mathrm{e}^{\lambda_2-\lambda_1(1-x)} \tag{A5, A6}$$

$$H_1^+(x,s)=\theta_0(s)\mathrm{e}^{\lambda_2 x-\lambda_1},\qquad H_1^-(x,s)=\mathrm{e}^{-\lambda_1(1-x)} \tag{A7, A8}$$

APPENDIX B: DERIVATION OF CONTROL FORCES

For $a_1 \leqslant x \leqslant d$, define

$$\hat{w}(x_1,s)\equiv\bar{w}(x_1,s)-\theta_0(s)\theta_1(s)\bar{w}(x_1,s), \tag{B1}$$

$$\hat{w}(x_2,s)\equiv\bar{w}(x_2,s)-\theta_0(s)\theta_1(s)\bar{w}(x_2,s), \tag{B2}$$

The following result can be established by applying equations (21) and (22) and simplifying the algebra:

$$\begin{aligned}
&\hat{w}(x_2,s)-\hat{w}(x_1,s)\mathrm{e}^{\lambda_2(x_2-x_1)}\\
&\quad=\left[G_U^+(x_2,a_2,s)+G_U^-(x_2,a_2,s)\right]\bar{q}_{a2}(s)+\left[G_D^+(x_2,a_1,s)+G_D^-(x_2,a_1,s)\right]\bar{q}_{a1}(s)\\
&\qquad+\left[G_U^+(x_2,d,s)+G_U^-(x_2,d,s)\right]\bar{f}_d(s)-\left[G_U^+(x_1,a_2,s)+G_U^-(x_1,a_2,s)\right]\bar{q}_{a2}(s)\mathrm{e}^{\lambda_2(x_2-x_1)}\\
&\qquad-\left[G_D^+(x_1,a_1,s)+G_D^-(x_1,a_1,s)\right]\bar{q}_{a1}(s)\mathrm{e}^{\lambda_2(x_2-x_1)}-\left[G_U^+(x_1,d,s)\right.\\
&\qquad\left.+G_U^-(x_1,d,s)\right]\bar{f}_d(s)\mathrm{e}^{\lambda_2(x_2-x_1)}\\
&\quad=\frac{1}{2s}(1-\theta_0(s)\theta_1(s)\mathrm{e}^{\lambda_2-\lambda_1})(1-\mathrm{e}^{(\lambda_2-\lambda_1)(x_2-x_1)})\mathrm{e}^{-\lambda_1(a_1-x_2)}\bar{q}_{a1}(s).
\end{aligned} \tag{B3}$$

Substituting equations (B1) and (B2) into equation (B3) and rearranging the result gives

$$\bar{q}_{a1}(s)=-\frac{2s[\bar{w}(x_2,s)-\bar{w}(x_1,s)\mathrm{e}^{\lambda_2(x_2-x_1)}]\mathrm{e}^{-\lambda_1(x_2-a_1)}}{1-\mathrm{e}^{(\lambda_2-\lambda_1)(x_2-x_1)}}. \tag{27}$$

For $d \leqslant x \leqslant a_2$, define

$$\hat{w}(x_3,s)\equiv\bar{w}(x_3,s)-\theta_0(s)\theta_1(s)\bar{w}(x_3,s), \tag{B4}$$

$$\hat{w}(x_4,s)\equiv\bar{w}(x_4,s)-\theta_0(s)\theta_1(s)\bar{w}(x_4,s), \tag{B5}$$

Then, the following result can be obtained:

$$\begin{aligned}\hat{w}(x_3, s) - \hat{w}(x_4, s)\mathrm{e}^{-\lambda_1(x_4-x_3)} &= [G_U^+(x_3, a_2, s) + G_U^-(x_3, a_2, s)]\bar{q}_{a2}(s) + [G_D^+(x_3, a_1, s) + G_D^-(x_3, a_1, s)]\bar{q}_{a1}(s) \\ &\quad + [G_D^+(x_3, d, s) + G_D^-(x_3, d, s)]\bar{f}_d(s) - [G_U^+(x_4, a_2, s) + G_U^-(x_4, a_2, s)]\bar{q}_{a2}(s)\mathrm{e}^{-\lambda_1(x_4-x_3)} \\ &\quad - [G_D^+(x_4, a_1, s) + G_D^-(x_4, a_1, s)]\bar{q}_{a1}(s)\mathrm{e}^{-\lambda_1(x_4-x_3)} - [G_D^+(x_4, d, s) \\ &\quad + G_D^-(x_4, d, s)]\bar{f}_d(s)\mathrm{e}^{-\lambda_1(x_4-x_3)} \\ &= \frac{1}{2s}(1 - \theta_0(s)\theta_1(s)\mathrm{e}^{\lambda_2-\lambda_1})(1 - \mathrm{e}^{(\lambda_2-\lambda_1)(x_4-x_3)})\mathrm{e}^{\lambda_2(x_3-a_2)}\bar{q}_{a2}(s). \end{aligned} \tag{B6}$$

Substituting equations (B4) and (B5) into equation (B6) and rearranging the result gives

$$\bar{q}_{a2}(s) = -\frac{2s[\bar{w}(x_3, s) - \bar{w}(x_4, s)\mathrm{e}^{-\lambda_1(x_4-x_3)}]\mathrm{e}^{\lambda_2(a_2-x_3)}}{1 - \mathrm{e}^{(\lambda_2-\lambda_1)(x_4-x_3)}}. \tag{28}$$

APPENDIX C: PROOF OF STABILITY THEOREM

Consider a system with the characteristic equation of $1 - \varphi(s)\mathrm{e}^{-\tau x} = 0$, where τ is positive real and s is complex. Substituting $\varphi(s) = r\mathrm{e}^{\mathrm{i}\alpha}$ and $s = \sigma + \mathrm{i}\omega$ into the characteristic equation gives

$$r\mathrm{e}^{-\tau\sigma}[\cos(\tau\omega - \alpha) - \mathrm{i}\sin(\tau\omega - \alpha)] = 1. \tag{C1}$$

Resolving the above equation into its real and imaginary parts leads to

$$r\mathrm{e}^{-\tau\sigma}[\cos(\tau\omega - \alpha)] = 1, \qquad r\mathrm{e}^{-\tau\sigma}[\sin(\tau\omega - \alpha)] = 0. \tag{C2, C3}$$

If $|\varphi(s)| < 1$ (thus $|r| < 1$), then from equation (C2), σ is negative real since τ is positive real and $|\cos(\tau\omega - \alpha)| \leqslant 1$. This implies that all poles of the system are located on the left half s plane. Therefore, the system is asymptotically stable when $|\varphi(s)| < 1$. On the other hand, if the system is asymptotically stable, σ must be negative real since all poles of the system are located on the left half s plane. To satisfy both equations (C2) and (C3), $|r| < 1$ which implies that $|\varphi(s)| < 1$. Moreover, if $\varphi(s)| = 1$, solving equations (C2) and (C3) leads to $\sigma = 0$, implying that the system is marginally stable since all poles lie on the imaginary axis of the s plane. However, if $|\varphi(s)| > 1$ (thus $|r| > 1$), then from equation (C2), σ is positive real since τ is positive real and $|\cos(\tau\omega - \alpha)| \leqslant 1$. This implies that all poles of the system are located on the right half s plane. Therefore, the system is unstable when $|\varphi(s)| > 1$. If the system is unstable, using the same procedure as for the asymptotic stability, it can be shown that $|\varphi(s)| > 1$.